Proc. Natl. Acad. Sci. USA
Vol. 83, pp. 2066–2070, April 1986
Biochemistry

Visualization of the paranemic joining of homologous DNA molecules catalyzed by the RecA protein of *Escherichia coli*

(electron microscopy/recombination/synapsis)

GUNNA CHRISTIANSEN* AND JACK GRIFFITH

Lineberger Cancer Research Center and Departments of Microbiology and Immunology and Biochemistry, University of North Carolina, Chapel Hill, NC 27514

Communicated by Mary Ellen Jones, December 2, 1985

ABSTRACT **In reactions catalyzed by the RecA protein of *Escherichia coli*, synapsis between two DNA molecules is believed to occur even in the absence of free homologous DNA ends and to involve a metastable interaction termed paranemic joining. We have used electron microscopic methods to visualize synapse formation between supertwisted M13 double-stranded DNA (dsDNA) and linear M13 mp7 single-stranded DNA (ssDNA) with non-M13 sequences at its ends. These non-M13 sequences block strand invasion and make this pairing equivalent to the joining of two fully circular molecules. We observed a high frequency of joining when the ssDNA was initially assembled into presynaptic filaments with RecA protein. Cleavage of the dsDNA in the joined complexes by *Hpa* I revealed that the joint was at a site of homology. In these joints, the dsDNA entered the presynaptic filament over a length of 360 ± 80 base pairs, not visibly altering its ultrastructure, and then dissociated from the filament. Although the dsDNA in the complexes appeared topologically relaxed, deproteinization released supertwisted dsDNA, indicating that the dsDNA was unwound by 34° per base pair in the paranemic joint. When supertwisted M13 dsDNA was paired with circular M13 ssDNA, similar joints were observed and both DNA circles appeared topologically relaxed.**

The electron microscopic visualization of D-loops produced in DNA by the action of the RecA protein of *Escherichia coli* (1, 2) is a landmark in studies of homologous recombination. In these reactions, RecA protein directs the invasion of a single-stranded DNA (ssDNA) end into a double-stranded DNA (dsDNA) in a region of homology. In these joints, as one strand of the dsDNA is displaced, the other base-pairs with the ssDNA, forming a hybrid double-helix (Fig. 1). These synaptic structures, termed plectonemic joints, are stable even after deproteinization, a property that has greatly facilitated their study. In particular, it has been shown that the action of RecA protein on a properly oriented plectonemic joint can directly lead to the complete exchange of strands between two DNA molecules (1–4).

It has been proposed that RecA protein can promote synapsis by a mechanism that does not require the presence of a free homologous DNA end (5). In this reaction (Fig. 1), all three strands of the DNAs are not topologically interwound, which causes these joints to be relatively unstable upon deproteinization and does not lead to productive strand exchange. The first experimental support for paranemic joining came from electron microscopic observations by DasGupta *et al.* (6) of rare RecA protein-dependent pairings of circular phage G4 dsDNA with circular M13 ssDNA containing a short insert of G4 sequence. Cunningham *et al.* (7) presented additional evidence of nonplectonemic DNA synapsis by showing that RecA protein and topoisomerase I could act on superhelical DNA and homologous circular ssDNA to topologically link the two DNAs. Bianchi *et al.* (5) demonstrated that paranemic joining occurred at a high frequency, and they estimated the size of the joints to be ≈500 base pairs (bp). More recently, Riddles and Lehman (8) have developed a filter binding assay that distinguishes paranemic joints from plectonemic joints by their relative lability to certain protein denaturants (e.g., 5.2 M guanidinium chloride). Julin *et al.* (9) have used this technique to follow the kinetics of paranemic joining. The observations that paranemic joints form rapidly (5, 9) and that nicking the ssDNA in paranemic synapses leads to plectonemic joint formation (6, 7) suggest that these structures may serve as precursors to plectonemic joints *in vivo*. Although little is known about the structure of paranemic joints, some investigators have suggested that all three DNA strands are wrapped about each other in the joint (10), and others have presented evidence that paranemic joints formed by the rec-1 protein of *Ustaligo* contain segments of left-handed DNA (11, 12).

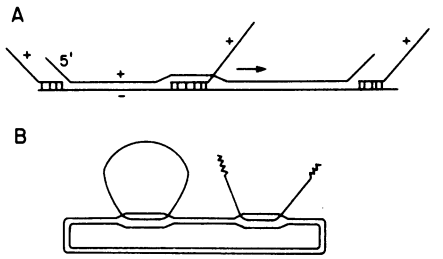

FIG. 1. Catalysis of joint formation by RecA protein. (*A*) When free homologous DNA ends are available, a linear ssDNA can form plectonemic joints at the ends or along the length of a homologous linear dsDNA. Arrow indicates the direction of strand exchange. (*B*) When the ssDNA and dsDNA are fully homologous but ends are absent (as at left) or when the ssDNA contains sequences at its ends that are not homologous to the dsDNA (as at right), less stable paranemic joints may form. In this case, the two DNAs are not topologically interlocked.

For RecA protein to catalyze synapsis, it must first assemble onto ssDNA to form a highly ordered complex termed a presynaptic filament. Recent studies in this and other laboratories (13–17) have examined this assembly process in detail. This information now makes it possible to use electron microscopy to examine the interaction of presynaptic filaments with dsDNA. In the study described here, we have used DNA substrates that can only join paranemically, and have been able to observe paranemic

The publication costs of this article were defrayed in part by page charge payment. This article must therefore be hereby marked "*advertisement*" in accordance with 18 U.S.C. §1734 solely to indicate this fact.

Abbreviations: ssDNA, single-stranded DNA; dsDNA, double-stranded DNA; SSB protein, single-strand binding protein; bp, base pair(s).

*On sabbatical leave from the Department of Medical Microbiology, University of Aarhus, Denmark.

joints at high frequency. This provides direct evidence for paranemic joining and allows us to distinguish among the several models that have been proposed.

METHODS AND MATERIALS

DNA and Proteins. M13 and M13 mp7 ssDNA and dsDNAs were prepared as previously described, including specific cleavage of the ssDNA using *Eco*RI endonuclease (17). RecA protein (18) and single-strand binding (SSB) protein (19) were purified as described.

Assembly of RecA Protein onto ssDNA and Joint Formation. RecA protein was assembled onto ssDNA as described (17). In brief, RecA protein (1 RecA monomer per 0.5–3 bases) in a 100 μl volume was preincubated with creatine phosphokinase (4 μg/ml; Sigma) and 20 mM creatine phosphate (Sigma) in 15 mM NaCl/3 mM ATP/0.1 mM EDTA/12 mM $MgCl_2$/20 mM Hepes buffer at pH 7.5 for 10 min at 37°C. ssDNA (6 μM nucleotide residues) was then added; 2 min later, 1 SSB protein monomer was added per 20 bases and incubation continued for 10 min at 37°C. At this point, the dsDNA was added to 6 μM and incubation continued for various times. These values correspond to the following concentration in the 100-μl reaction volume: ssDNA, 2 μg/ml; dsDNA, 4 μg/ml; RecA protein, 80–300 μg/ml; SSB protein, 6 μg/ml. The samples were then fixed with formaldehyde and glutaraldehyde (20) at 20°C. Free and complexed DNA molecules were separated from free proteins by chromatography on Sepharose 4B. Unfixed samples were deproteinized with 0.1% $NaDodSO_4$ at 37°C for 2 min and then separated from the detergent and free proteins by chromatography on Sepharose 4B.

Electron Microscopy. Samples to be visualized directly were fixed, adsorbed to thin carbon films in a buffer containing spermidine, dehydrated through a graded series of ethanol washes, air-dried, and rotary shadowcast with tungsten as described (20). Samples to be visualized by surface spreading in 40% (vol/vol) formamide were prepared as described by Christiansen and Christiansen (21). Micrographs were taken on a Philips EM400 TLG and lengths were determined by direct tracing from the negatives, using a Summagraphics digitizer coupled to an Apple II computer.

RESULTS

Visualization of Paranemic Joining Between Linear ssDNA and Supertwisted dsDNA. Supertwisted M13 dsDNA and linear M13 mp7 ssDNA that is cleaved at the center of the 830-base *lac*-polylinker insert represent DNA molecules that can only join paranemically. This cleavage places 400 bases of non-M13 sequences at each end of the ssDNA. These nonhomologous sequences block strand-invasion by the ssDNA, allowing this template pair to mimic paranemic joining by two fully circular DNA molecules. Below we describe the joining of these DNAs catalyzed by RecA protein.

For these experiments, linear M13 mp7 ssDNA was first assembled into presynaptic filaments with RecA protein in the presence of Mg^{2+}, ATP, and SSB protein (*Methods and Materials* and ref. 17). The ssDNA in the presynaptic filaments is fully covered by RecA protein from the 3′ end to within a short distance of the 5′ end, which remains covered by undisplaced SSB protein (17). Supertwisted M13 dsDNA was then added at a 1:1 molar ratio and incubation continued. The resultant DNA–protein complexes then were either deproteinized with 1% $NaDodSO_4$ and the DNA examined by surface-spreading electron microscopy or were fixed and visualized directly.

Examination of the deproteinized DNA at all time points revealed that only supertwisted dsDNA and full-length linear ssDNA were present. Thus, the DNA could not have been nicked during the incubation, since no plectonemic joints were formed. When the dsDNA and presynaptic filaments were incubated together for 10 min then fixed and visualized directly by electron microscopy, >75% of the dsDNA molecules were found paired with single presynaptic filaments over a short distance (Fig. 2 *A* and *B*). The dsDNA in the joined complexes appeared topologically relaxed, or showed at most 1–3 crossovers, and was bound to the presynaptic filament at only one site. Measurement of many complexes showed that joining occurred at random distances from the ends of the presynaptic filaments except at the very ends (data not shown). This result was expected since the ssDNA ends lack homology with the dsDNA. At the joint, the dsDNA entered into the 10-nm-diameter presynaptic filament for a short distance, then exited the filament without visibly altering its ultrastructure. When superhelical pBR322 dsDNA was incubated with presynaptic filaments formed with M13 mp7 ssDNA, no joints were found.

To follow the kinetics of joint formation, the dsDNA and presynaptic filaments were incubated together for 30 sec to 45 min, fixed, and mounted directly for electron microscopy. One hundred dsDNA molecules were scored for being present in singly joined complexes, in aggregates containing three or more molecules, or as free supertwisted dsDNA. After a 30-sec incubation, 74% of the dsDNA molecules were in singly joined complexes, 14% were in aggregates, and 12% were scored as free supertwisted dsDNA. From 1 min to 10 min of incubation, 70–75% of the dsDNA molecules were in singly joined complexes, 8% were in aggregates, and 20% were free supertwisted dsDNA. After a 45-min coincubation, 42% of the dsDNA molecules were in singly joined complexes, 2% were in aggregates, and 56% were scored as free supertwisted dsDNA. Thus we conclude that under these conditions, paranemic joining occurs very rapidly and the fraction of joined complexes remains high until the point at which the ATP-regenerating enzymes have likely begun to lose their activity.

The average length of 26 joints was 0.09 ± 0.02 μm or 360 bp, assuming a value of 3.0 Å/bp (22). Similar joined complexes were observed when the fixed complexes were surface-spread in the presence of 40% formamide (Fig. 2*C*). However, the length of the presynaptic filaments in the surface-spreads reproducibly measured 125% the length of the equivalent protein-free dsDNA, as contrasted to 80% when they were prepared by the direct-mounting methods. Measurement of the length of 15 joints prepared by this method gave a value of 0.15 ± 0.04 μm. When the length extension was taken into consideration, this also yielded a length of 360 bp involved in the paranemic joints. In previous work (23), counting of bands resolved by agarose gel electrophoresis showed that M13 dsDNA prepared by the methods used here has 35 ± 3 superhelical twists (23). Thus 360 bp is very close to the 367 bp of the superhelical M13 dsDNA that, if melted, would just relax its 35 natural supertwists [based on 10.5 bp per turn in natural dsDNA (22, 24)].

To extend this apparent correlation between the length of the joint and the number of superhelical turns of the dsDNA, an 11.6-kbp dsDNA construct consisting of M13 mp19 with a 4.3-kbp insert of *E. coli* DNA (gift of Tai-Ping Sun, Duke University) was paired with M13 ssDNA. When this was done, joints were observed that measured 0.20 ± 0.006 μm (n = 14) by direct mounting or 0.25 ± 0.007 μm (n = 33) after spreading in 40% formamide. These values calculate to 780 and 600 bp, respectively. The 11.6-kbp dsDNA would have ≈63 supertwists (based on its proportionately greater size and 35 supertwists for M13 dsDNA) whose relaxation would require the melting of 670 bp. As long as we assume that the

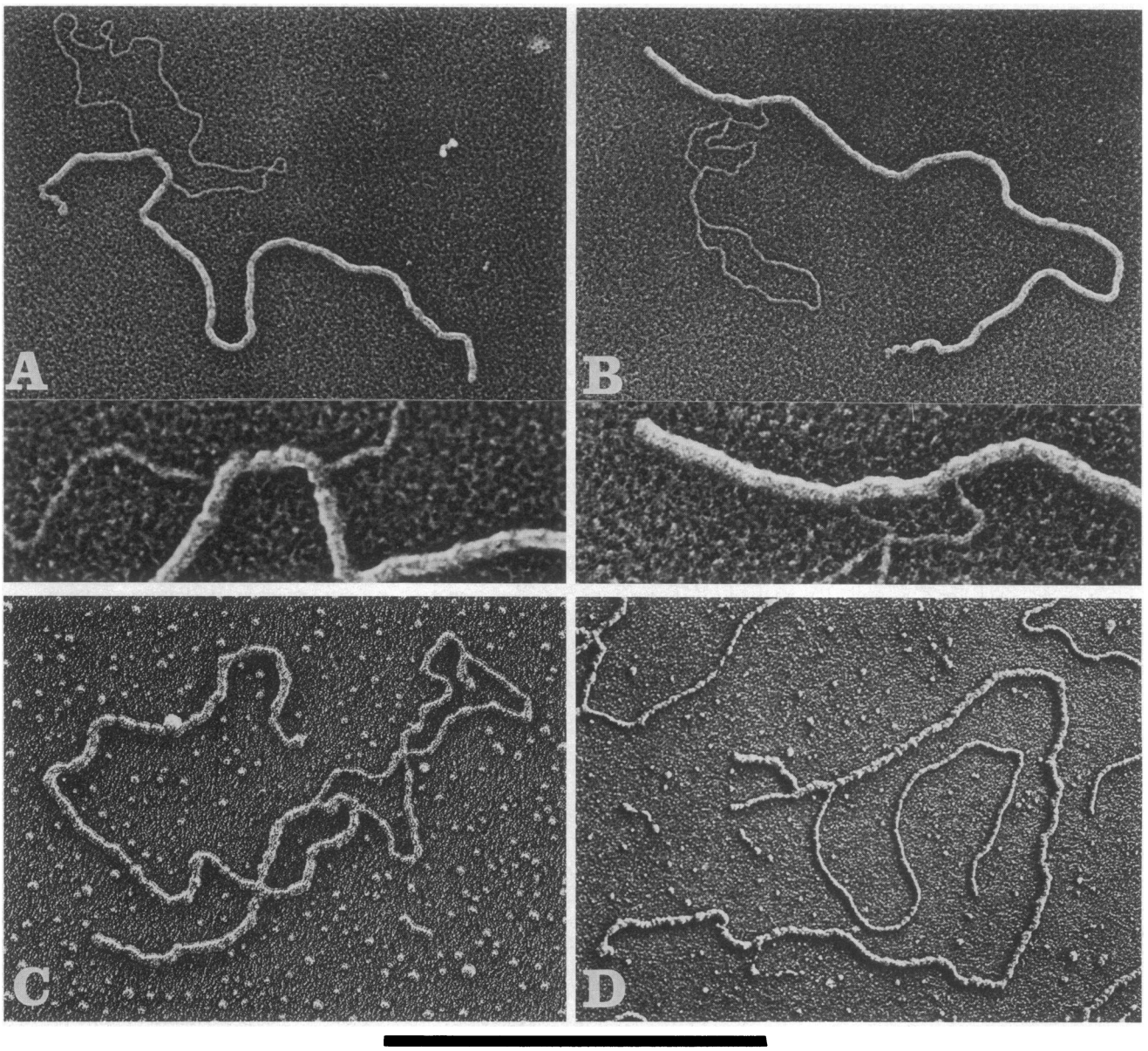

FIG. 2. Visualization of paranemic joining. Superhelical M13 dsDNA was incubated with presynaptic filaments formed by RecA protein binding to linear M13 mp7 ssDNA (cleaved in the *lac*-polylinker insert). After incubation, the samples either were fixed, adsorbed directly to thin carbon films, and shadowcast with tungsten (*A* and *B*) or were fixed and spread from 40% formamide onto a 10% formamide solution in the presence of cytochrome *c* (*C* and *D*). Higher magnifications in *A* and *B* are enlargements of the joints in the molecules above. Note that joining unwinds the superhelical twists of the dsDNA. In *D*, the dsDNA was cleaved with *Hpa* I prior to spreading. The ends of the dsDNA and ssDNA are colinear to within 10% (see text). Bar = 1 μm (*A–D*) or 0.3 μm (enlargements).

dsDNA is neither compacted nor extended in the joint, this correlation suggests that the two strands of the dsDNA are just held apart in the joint.

Pairing Is at a Site of Homology. It was essential to demonstrate that the paranemic joints we observed formed at sites of homology. This required cleaving the dsDNA after pairing at a site as close as possible to the M13 map position at which the ssDNA had been cut. Synapsis at homologous sites would produce complexes with equal-length ssDNA and dsDNA arms. The dsDNA in the joined complexes can be cleaved with restriction endonucleases after the proteins have been fixed in place, as long as the complexes are chromatographed on Sepharose 4B to remove the fixatives. M13 dsDNA has a single *Hpa* I site 539 bp from the site into which the 830-bp *lac*-polylinker segment was inserted to generate M13 mp7. When the M13 sequences of an *Hpa* I-cut M13 dsDNA molecule are aligned with those of an *Eco*RI-cut M13 mp7 ssDNA, at one end the dsDNA extends past the ssDNA by 177 bp (2% of the total length), while at the other end the ssDNA extends beyond the dsDNA end by 965 bases (13%). If we arbitrarily reduce the length of the linear M13 mp7 ssDNA by 415 bases, then the coincidence at each end of the two aligned molecules should be within 8% of their total length. Joined complexes were prepared, fixed, chromatographed on Sepharose 4B, treated with *Hpa* I, and then visualized directly (not shown) or visualized by surface-spreading in the presence of 40% formamide (Fig. 2*D*). The latter method provided a convenient means for measuring the lengths of the DNA arms in each complex, as the four arms were well separated. When the length of the shorter presynaptic arm (as measured in formamide spreads) was reduced by 415 bases, corrected for its greater length after surface-spreading, and then compared to the length of the short dsDNA arm in the same complex, the ratio (ssDNA arm/dsDNA arm) was 1.00 ± 0.15 (n = 13). This ratio and small standard deviation in spite of the fact that the joints

were found in all distances from the DNA ends could have only resulted from the joints being at sites of homology.

Visualization of Paranemic Joining Between Homologous ssDNA and dsDNA Circles. Due to the lack of ends, circular ssDNA can only join paranemically with homologous circular dsDNA. It was important to determine whether the joints formed with these substrates are similar to those previously seen and whether the two DNAs are highly supercoiled about each other as predicted by some models of paranemic joining (10). Presynaptic filaments were formed with RecA protein and circular M13 mp7 ssDNA. Supertwisted M13 mp7 dsDNA was then added and incubation continued for 10 min. When aliquots of these reactions were deproteinized and examined by surface-spreading electron microscopy in 40% formamide, unjoined supertwisted dsDNA and circular ssDNA molecules were seen almost exclusively. A 0.5% level of linear ssDNA joined to open circular dsDNA (in the form of D-loops) was observed, but this value also represented the fraction of linear ssDNA contaminating the circular ssDNA preparation. When identical aliquots were fixed and either visualized directly or by surface-spreading, circular presynaptic filaments bound to dsDNA circles were found in abundance. Although the presynaptic filaments were open and untwisted (Fig. 3 *A* and *B*) and the dsDNA appeared topologically relaxed, they were often intertwined, making it difficult to determine whether joining had occurred at more than one site. However, when the dsDNA in the fixed complexes was cleaved with *Hpa* I, the DNAs were seen to be joined only once (Fig. 3 *C* and *D*). The appearance of the joints was similar to that observed above and their length measured 300 ± 100 bp (n = 10).

DISCUSSION

In this paper we present direct electron microscopic evidence of paranemic joining between homologous DNA molecules catalyzed by RecA protein. Under optimal conditions and with DNA substrates incapable of forming plectonemic joints, up to 75% of the DNA molecules were found in complexes containing one superhelical dsDNA joined to one

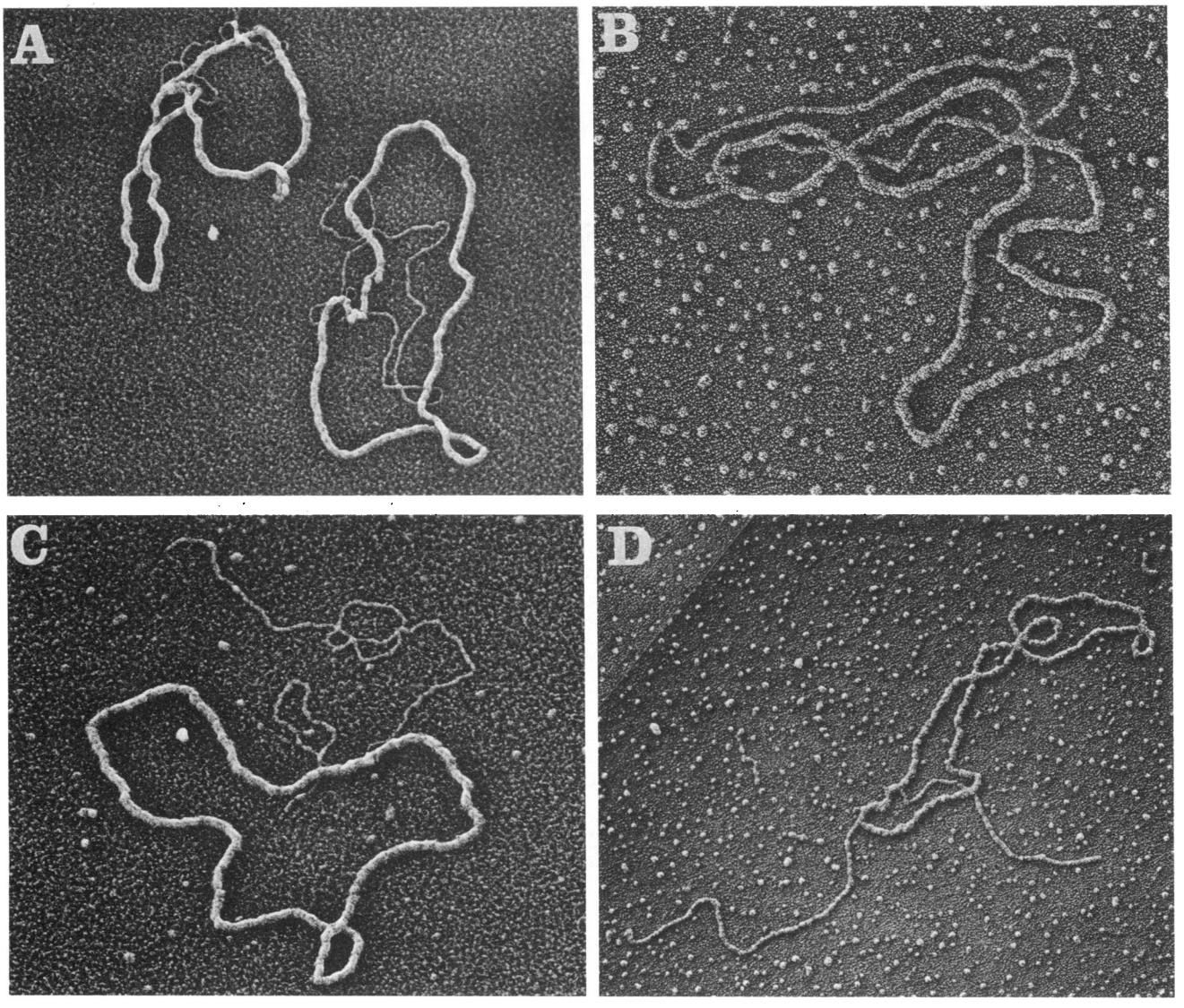

FIG. 3. Visualization of paranemic joining between circular DNAs. Superhelical M13 mp7 dsDNA was incubated with presynaptic filaments formed by RecA protein binding to circular M13 mp7 ssDNA. Samples were fixed and either examined directly after shadowcasting with tungsten (*A* and *C*) or spread from a 40% formamide solution onto a 10% formamide solution in the presence of cytochrome *c* (*B* and *D*). In *C* and *D*, the dsDNA was cleaved with *Hpa* I after fixation of the samples. The lack of superhelical turns in either the dsDNA or the presynaptic filaments is particularly apparent in *B*. Bar = 1 μm (*A* and *B*), 0.67 μm (*C*), or 1.5 μm (*D*).

RecA protein-covered ssDNA at a single site. At the joint, the dsDNA, which appeared topologically relaxed, disappeared into the RecA protein–ssDNA filament for a short distance and then reappeared without visibly altering the ultrastructural appearance of the presynaptic filament. The length of the joint corresponded to the length of the dsDNA that, if completely melted, would just unwind its natural superhelical turns.

We employed superhelical dsDNA in order to measure changes in topology resulting from synapsis. Here, the length of the joints did not grow beyond the point at which the dsDNA would have begun to acquire positive superhelical twists. Utilization of linear dsDNAs or DNA gyrase might serve as a means to circumvent any constraints imposed by superhelicity. The rate of dissociation of the paranemic joints (the rate of formation was very rapid) and whether the joints can move along the dsDNA remain to be determined.

Our results are in good agreement with those of Bianchi *et al.* (5), who found that paranemic joints formed rapidly and remained stable when an ATP-regeneration system was employed. Direct measurements of the length of the joints closely approximate their estimate of 500 bp within the joints as derived from nuclease-sensitivity studies. The lability of these joints after deproteinization, the kinetics of their formation, and the 70–90% extent of joining that we observed all correlate well with the studies of Lehman and his colleagues (8, 9). The unwinding of the dsDNA in each paranemic joint measured here is less, by a factor of ≈3, than the estimated 1000 bp or more derived by indirect means by Wu *et al.* (25). Even at incubation times as short as 30 sec, the dsDNA always appeared relaxed. If a precursor to paranemic joining exists (9) in which the dsDNA is not fully unwound, it must be very short-lived.

Our results provide several important constraints on models of paranemic joints: (*i*) this structure must be dominated by the architecture of the presynaptic filament, since no visible change in the ultrastructure of the joint was observed due to the presence of the dsDNA; (*ii*) no solenoidal twisting of the ssDNA or dsDNA outside the joint is induced by paranemic joining; and (*iii*) the dsDNA in the joint must unwind by an amount equivalent to the complete separation of the two strands. This unwinding, 34° per bp, is the same amount that would result from the formation of a plectonemic joint. Indeed, we have observed (unpublished results) that plectonemic and paranemic joints with RecA protein bound appear indistinguishable as visualized by electron microscopy. Although it is possible to draw schematics (e.g., Fig. 1) of how the DNA strands are arranged in a plectonemic joint, their physical arrangement within the RecA protein filament remains unknown. Thus it is even more difficult to propose models for the ultrastructure of paranemic joints, since the manner in which the three strands can interact in the absence of protein is uncertain. However, if in a paranemic joint the three DNA strands within the RecA protein filament are separated into a duplex DNA segment and a ssDNA segment, then the topological constraints on paranemic joints elucidated here argue that the duplex DNA segment may exist in alternating left-handed and right-handed turns as suggested by Kmiec and Holloman (11, 12).

It has been convenient both to consider strand-exchange *in vitro* as a series of discrete steps and to utilize factors and DNA substrates that make it possible to isolate these steps for study. Such studies promote the impression that each step involves the formation of a new RecA protein–DNA structure. Our observation that the ultrastructure of paranemic joints is very similar to that of presynaptic filaments (and to plectonemic joints) supports a different view. We suggest that a single RecA protein filament serves as the basic scaffold upon which a continuous process, from the initial search for homology to the final events of strand exchange, is orchestrated.

We thank Jim Register and Randy Thresher for helpful discussion and editorial efforts and Sheila Colby for preparation of RecA and SSB proteins. This work was supported in part by Grant GM31819 from the National Institutes of Health and Grant CA16086 from the National Cancer Institute. Travel by G.C. was supported in part by a grant from the Danish Medical Research Foundation.

1. McEntee, K., Weinstock, G. M. & Lehman, I. R. (1979) *Proc. Natl. Acad. Sci. USA* **76**, 2615–2619.
2. Shibata, T., DasGupta, C., Cunningham, R. P. & Radding, C. M. (1979) *Proc. Natl. Acad. Sci. USA* **76**, 1638–1642.
3. Cox, M. M. & Lehman, I. R. (1981) *Proc. Natl. Acad. Sci. USA* **78**, 6018–6022.
4. Kahn, R., Cunningham, R. P., DasGupta, C. & Radding, C. M. (1981) *Proc. Natl. Acad. Sci. USA* **78**, 4786–4790.
5. Bianchi, M., DasGupta, C. & Radding, C. M. (1983) *Cell* **34**, 931–939.
6. DasGupta, C., Shibata, T., Cunningham, R. P. & Radding, C. M. (1980) *Cell* **22**, 437–446.
7. Cunningham, R. P., Wu, A. M., Shibata, T., DasGupta, C. & Radding, C. M. (1981) *Cell* **24**, 213–223.
8. Riddles, P. W. & Lehman, I. R. (1985) *J. Biol. Chem.* **260**, 165–169.
9. Julin, D. A., Riddles, P. W. & Lehman, I. R. (1985) *J. Biol. Chem.*, in press.
10. Howard-Flanders, P., West, S. C. & Stasiak, A. (1984) *Nature (London)* **304**, 215–220.
11. Kmiec, E. B. & Holloman, W. K. (1984) *Cell* **36**, 593–598.
12. Kmiec, E., Kroeger, P., Holliday, R. & Holloman, W. (1984) *Cold Spring Harbor Symp. Quant. Biol.* **49**, 675–682.
13. Cox, M. M. & Lehman, I. R. (1982) *J. Biol. Chem.* **257**, 8523–8532.
14. Kahn, R. & Radding, C. M. (1984) *J. Biol. Chem.* **259**, 7495–7503.
15. Flory, J., Tsang, S. S. & Muniyappa, K. (1984) *Proc. Natl. Acad. Sci. USA* **81**, 7026–7030.
16. Griffith, J., Harris, L. D. & Register, J. C. (1984) *Cold Spring Harbor Symp. Quant. Biol.* **49**, 553–559.
17. Register, J. C. & Griffith, J. (1985) *J. Biol. Chem.*, in press.
18. Griffith, J. & Shores, C. G. (1985) *Biochemistry* **24**, 158–162.
19. Chase, J. W., Whittier, R. F., Auerbach, J., Sancar, A. & Rupp, W. D. (1980) *Nucleic Acids Res.* **8**, 3215–3227.
20. Griffith, J. & Christiansen, G. (1978) *Annu. Rev. Biophys. Bioeng.* **7**, 19–37.
21. Christiansen, G. & Christiansen, C. (1983) *Nucleic Acids Res.* **11**, 37–56.
22. Griffith, J. (1978) *Science* **201**, 525–527.
23. Sperazza, J. M., Register, J. C. & Griffith, J. (1984) *Gene* **31**, 17–22.
24. Wang, J. (1979) *Proc. Natl. Acad. Sci. USA* **76**, 200–203.
25. Wu, A. M., Bianchi, M., DasGupta, C. & Radding, C. M. (1983) *Proc. Natl. Acad. Sci. USA* **80**, 1256–1260.